Mathematical Modelling and Computational Dynamics: A data-driven Analysis of impact of Quasi-Lockdown Policy in Control of COVID-19 in Akwa Ibom State, Nigeria

Authors' contributions

All authors contributed effectively in writing of this paper. All authors read and approved the final manuscript

Original Research Article

Abstract

Determining the impacts of a local control strategy, implemented to curtail the spread of COVID-19 has become obligatory to enable policy makers in preparation to combat the so-called long covid. This research used a deterministic SEIAHR-model, incorporating a logistic function to investigate the effect of quasi-lockdown policy during re-emergence of corona virus pandemic. The notion of uniform convergence and fixed point theory were used to establish positive invariant region, ultimate boundedness, and existence of unique solution of the model. Nonlinear dynamical behaviours of the model such as stability and oscillating flows occurred at the disease free, and endemic equilibrium points. Using centre manifold theory, a trans-critical bifurcation with hysteresis effect were established, when quasi-lockdown policy was used as a control parameter in the model. A forward sensitivity analysis was conducted to unfold parameters that contributed significantly towards the spread and control of the infection. These parameters were estimated and fitted using least square technique, comparative to the observed real datasets adapted from the Nigeria Centre for Disease Control (NCDC). The polynomial regression model fitted the observed datasets with an average coefficient of determination given as $R^2 = 0.94$. Simulations in form of phase space diagrams were used to validate the theoretic results.

Epidemiologically, the model demonstrated that quasi-lockdown policy was necessarily a strategic policy to curb the spread of the infection, but not sufficient to eradicate the disease as the disease persisted endemically. It was shown that the basic reproduction number of the infection was within the critical threshold ($R_0 \leq 1$), when the lockdown policy was enforced strictly, but otherwise on its relaxation of the lockdown policy ($R_0 > 1$). Thus a relaxation of the quasi-lockdown policy leads to increase in susceptibility of the populace as the infection risk ratio increases in the model. Similarly, the model predicted that a pre-mature lifting of the lockdown policy could have led to high infectivity on the susceptible class and disastrous to healthy living of the citizens.

Keywords: COVID-19, mathematical modelling, computational dynamics, and quasi-lockdown policy

2010 Mathematics Subject Classification: 53C25, 83C05, 57N16.

1.0 Introduction

Emergence and re-emergence of infectious diseases such as corona viruses are integral part of the natural ecological system. Coronaviruses (CoVs) are lethal zoonotic viruses, which belong to nidovirales order, coronaviridae family, and coronavirinae subfamily. They are classified into five generations, namely alpha-coronavirus, beta-corona virus, gamma-corona virus, delta-corona virus and omicron-corona virus, by phylogenetic analyses and genomic relationships [1]. Major evolutionary models shown that CoVs of each genus are found in diverse animal species including horses, bats, cows, pigs, dogs, cats, birds, and ferrets. They are highly pathogenic in nature, forming the etiological agent of diseases in humans, ranging from common cold to severe illnesses such as Middle East Respiratory Syndrome (MERS-COVs) and Severe Acute Respiratory Syndrome (SARS-COVs), enteric, renal, neurological, and other diseases [2]. Recently, an infectious pathogen of severe acute respiratory syndrome corona virus-2 (SARS-COV-2), had emerged in Wuhan of China, termed COVID-19. It was a viral infection that affected breathing and blockage of the nostrils, throat, bronchi and lungs. The incubation period of COVID-19 has been approximated to have a mean, median, and mode of 7.83, 7, and 5 days, and, in 12.5% of cases, more than two weeks [3]. It was characterized by sudden onset of high fever, aching muscles, headache, kidney failure, severe malaise, non-productive cough, sore throat,rhinitis, pneumonia, decrease in leukocyte counts, cytokine storm, and sudden death in severe cases. The virus was mainly transmitted easily from person to person via droplets and small particles produced when infected people cough or sneeze. SARS-COV-2 virus tends to spread rapidly and has become a seasonal epidemic. Its new strain considered as corona virus (COVID-19) has been contagious and killed more than 6.9 million people with co-morbidity.

In Nigeria, the index case of the virus appeared on the 20th February, 2020 in Lagos, as announced by the Nigeria Centre for Disease and Control (NCDC), and had since spread sporadically to other parts of the Federation including Akwa Ibom State [4, 5]. This propelled the government to take devastating measures such as the declaration of a total lockdown; closure of schools and businesses, including restriction of international and local travelling in the country. The pandemic reaches its epic in August, 2022 in Nigeria between week 35-36, before declining, without any death case reported in 2023. The bi-weekly epidemiologoical reports of the NCDC, as at 26th February, 2023 shown a cumulative active infected cases of 266,313 and 3,155 deaths (case confirmed fatality rate (CFR) of 1.2%) in the country. On the other hand, in Akwa Ibom state a total of 5010 confirmed case with death cases of forty four (44) has been reported by NCDC since the outbreak of the pandemic. The first wave of COVID-19 in Akwa Ibom State witnessed the adoption of some strategic programmes to curtail the spread of the infection such as embacking on Flexible Educational Programmes(FEPs) [6, 7, 8]. This entails the synchronous and synchronous learning platforms for school children restricted by closure of schools, distance learning programmes and public health sensitization campaigns on the use of non-pharmaceutical interventions. Personal Protective Measures (PPMs) used were (a) avoiding contagious people of related symptoms, and complete social distancing(i.e., being at 2m in proximity to susceptible individuals), (b) washing of hands for at least 20 seconds, (c) using of sanitizers with at least 60% of alcohol, (d) disinfecting surfaces, and frequently

touched objects, and (e) isolation of suspected infected individuals. As part of the use of Personal Protective Measures (PPMs), the government recommended and provided personal protective equipment such as use of face masks, use of hand gloves with personal protective clothing by healthcare workers while giving care to COVID-19 patients and other response mechanisms [9].

In the long run, therapeutic interventions, treatments and vaccinations became common through effort of scientific and biomedical researches[10]. Different pharmaceuticals passed ethically approved clinical trials under the Monitored Emergency Use of Unregistered Interventions System (MEURI), with strict supervision [11]. Inspite of human immune activators to reduce the viral loads, drugs were utilized to moderate the prevalence, virulence, and molecular evolution rate of the infection. Several investigatory drugs and immune modulator drugs such as chloroquine, nitazoxanide, and ribavirin in combination of PEGylated interferon alfa-2a and -2b have shown inhibitory action against SARS-CoV-2 infection [12], as shown in figure 1

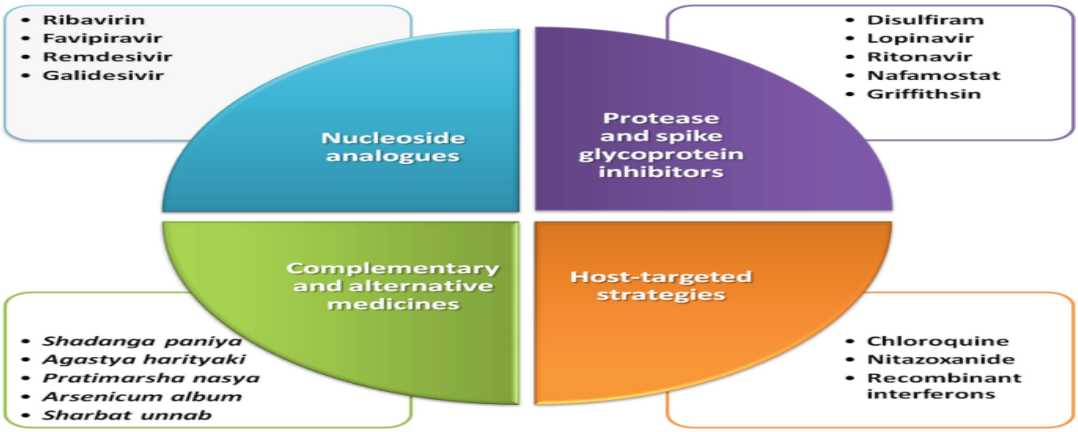

Figure 1: Investigational treatment approaches of COVID-19

In Akwa Ibom state, 63,336, and 69,030 doses of Moderna and AstraZeneca vaccines were received respectively. The Akwa Ibom State Ministry of Health in an emergency covid-19 report on August, 2021 has it that, about 14% and 95% of the two brands of vaccines were administered respectively. These interventions were very strategic in managing and controlling the spread of the infectious disease, but it becomes a necessity to assess the effectiveness of these measure in preparation for subsequence occurrence.

Empirically, mathematical and computational modelling remain instrumental to analyse the impacts of such infectious disease. Mathematical modelling has been used to investigate the dynamical behaviour and control measures of COVID-19 [13] in the presence of delta and omicron with vaccination and non-pharmaceutical interventions. They unfolded that omicron variant is more transmissible than other variants. They recommended a continued combination of non-pharmaceutical interventions with vaccination programs to control the disease outbreak. The impact of vaccination strategies on the spread of COVID-19 has been investigated in [14], via mathematical modelling approach. Based on the results from sensitivity analysis, they opined that vaccination rate, contact tracing, rapid testing are the most important parameters that reduced the effective reproduction number of the virus. Analogously, the impact of testing and isolation compliance on the transmission of COVID-19 in its early stage was investigated in [15]. Using the qualitative properties of the model, they highlighted that the daily infection peak showed high testing rates and high isolation compliance reduced the prevalence of the infection remarkably. In the same vein, a classical Susceptible, Exposed, Infected and Recovery (SEIR)-Model

[16] has been modified to incorporate compartments for vaccinated, asymptomatic, hospitalized, and deceased individuals. Through the alteration of the modelling parameters, it was revealed that vaccination rate, immunity loss, and relaxation of measures regarding the vaccinated individuals affect the dynamics of COVID-19 spread. There was an exponential increase in the death rate during the dominance of the delta variant and before the initiation of the booster shot program. Also, the co-dynamical properties of COVID-19 and tuberculosis has been investigated in [17] , and a deterministic inversion reproduction of the two infectious diseases were obtained. Using numerical simulation of the fitted datasets, they reported that COVID-19 incidence decreases with co-infection prevalence, then the burden of tuberculosis on the human population increases. Using the optimal control theory in [18] , a combination of the effect of COVID-19 vaccination and exogenous reinfection for tuberculosis(TB). In the analytic result, reducing the basic reproduction ($R_0 < 1$) was not sufficient to eliminate the disease from the community, because of co-morbidity of COVID-19, with tuberculosis (TB). In-spite the foregoing models, this paper proposes a much more realistic data-driven model of transitions, transmission and control of the infectious disease, with logistic function as per capita influx varying functional to control the susceptibility and infectivity of the system.

1.1 Model Description and Formulation

Considering the total population of individuals at time t, $N(t)$, and sub-populations as (a) Total susceptible individuals to COVID-19 at time t, $S(t)$. This includes the total infectious individuals limited by quasi-lockdown measure within the entire population. (b) Total exposed individuals to COVID-19 at time t, $E(t)$. This entails numerous front-line health-workers, and people at high risk of contracting the infection, after due contact with any infected persons (with and without any visible symptoms). (c) Total asymptomatic infected class of individuals with COVID-19 at time t, $A(t)$. This connotes individuals that are infectious to others without any visible symptoms of the infection after contact tracing programme. They are assumed to have high immune efficacy to suppress and delay the viral loads of the infection, and can recovered from the infection without treatment. The asymptomatic class of individuals, may have exceeded the initial incubation period (i.e., seven to fourteen days) of the infection (d) Total infected and infectious individuals with COVID-19 at time t, $I(t)$. This population registered the incident case of COVID-19 in the entire population. In this model, the total active cases of the population with COVID-19 is derived from NCDC, during the epic-week of the infection in Akwa Ibom State, see figure 2) (e) Total hospitalized individual with COVID-19 at time t, $H(t)$. This population is quarantined, and get treated of the infection after being diagnosed of symptoms of COVID-19. They were quarantine or self-isolated for treatment and (f) Total individuals that recovered from COVID-19, after treatment or through immune efficacy, at time t, $R(t)$. For biological relevance, all subpopulations are subject to positive initial population, and the entire population is represented in a functional space region given in equation (1.1)

$$\begin{cases} N(t) = & S(t) + E(t) + A(t) + I(t) + H(t) + R(t) | (S(t), E(t), A(t), I(t), H(t), R(t)) > 0 \\ & S(t) = S_0, E(t) = E_0, A(t) = A_0, I(t) = I_0, H(t) = H_0, R(t) = R_0, \forall\, t \geq 0 \\ & S_0 > 0, E_0 > 0, A_0 > 0, I_0 > 0, H_0 > 0, R_0 > 0 \\ \Omega \quad = & (S(t), E(t), A(t), I(t), H(t), R(t)) \in \mathbb{R}^6_+ | 0 \leq N(t) \leq N_{max} \end{cases} \tag{1.1}$$

Equation (1.1) defines a positive invariant region, well possedness, and boundedness of the model for epidemiological relevance. It forms a solution space as Ω-attractor set of plausible dynamics of COVID-19 pandemic. Hence solution that are in the Ω remains in $\Omega\ \forall\ t \geq 0$. Using the state variables of the model, the targeted population $N(t)$ can be recruited to the susceptible class of individuals via a logistic growth function $\alpha S(t)\left(1 - \frac{S(t)}{\kappa}\right)$. There is a restriction in the population of the susceptible class based on rumours of spontaneous spread of the infection, and enforcement of total lockdown using the parameter, κ. The parameter, α measures the recruitment rate from the targeted population to the susceptible class of individuals, due to natural birth rate or immigration. The transmission rate from susceptible class to symptomatically infected class, and exposed class are denoted

by β and μ respectively. Almost all exposed individuals are transfered to the infected class and asymptomatic class by the fractions $\epsilon(1-\rho), \rho \neq 1$, and $\epsilon\rho$ respectively, where ϵ is the transmission rate. The parameter ρ depicts an adjustment for uncertainty in proportional movement, after contact tracing. The rate in which the infected class of individuals are transferred to the hospitalized class is denoted by ψ, with recovery rate, η. Also, the asymptomatic individuals recover at the rate δ, and transferred to the recovery class. Each subpopulation, namely susceptible, exposed, asymptomatic, infected, hospitalized, and recovery classes, decreases by the natural death rate, denoted by σ, respectively. The COVID-19 induced death rate for exposed, asymptomatic, infected, and hospitalized individuals are denoted by ϱ, ζ, ν and ω respectively. The assumptions of the model include the following:

- The targeted population is non-homogeneous, as there is restriction on the carrying capacity, where the susceptible class can be infected or exposed to the pandemic. This implies that some individuals had already practiced self-isolation, before the epi-week of the infection in the state.
- The model incorporates uncertain parameter (ξ) on the fatality rate of the infection as some persons that died naturally were attributed to co-morbidity in COVID-19 after recovery from the infection. Thus, individuals in each group have equal natural death rate, excluding the recovery class of individuals.
- Proportionate movement of exposed class of individuals to infected and asymptomatic class of individuals respectively.
- The model datasets are estimated using the NCDC bi-weekly epidemiological report of COVID-19 peculiar to Akwa Ibom State, between 1st to 30th August, 2021.
- Zoonotic infectiousness of the viral disease has been neglected.

The proposed mathematical model that depicts the nonlinear dynamics; transmission and transfer within the subpopulations leads to the following system of ordinary differential equation 1.2. The model in equation (1.2) is subject to the initial condition in equation (1.1).

$$\begin{cases} \frac{dS}{dt} = & \alpha S(t)\left(1-\frac{S(t)}{K}\right) - \beta S(t)E(t) - \mu S(t)I(t) - \sigma S(t) \\ \frac{dE}{dt} = & \beta S(t)E(t) - \epsilon E(t) - (\varrho+\sigma)E(t) \\ \frac{dI}{dt} = & \mu S(t)I(t) + \epsilon\rho E(t) - \psi I(t) - (\zeta+\sigma)I(t) \\ \frac{dA}{dt} = & \epsilon(1-\rho)E(t)) - \delta A(t) - (\nu+\sigma)A(t) \\ \frac{H}{dt} = & \psi I(t) - \eta H(t) - (\omega+\sigma)H(t) \\ \frac{dR}{dt} = & \delta A(t) + \eta H(t) - (\xi+\sigma)R(t) \end{cases} \tag{1.2}$$

Epidemiological interactions of the state variables and parameters is given in figure (2). The following theorem is used to establish the boundedness of the epidemiological parameters within positive invariant region.

1.2 Uniform Convergence in COVID-19 Model

Theorem 1 [19]: Define a time-dependent vector space of the model in equations (1.1) and (1.2) as $\boldsymbol{X} = (S(t), E(t), A(t), I(t), H(t), R(t))^T$ on a continuously differentiable functional $\boldsymbol{F} \in C^1$ such that $\boldsymbol{F} : \boldsymbol{J} \times \boldsymbol{R}^6_+ \to \boldsymbol{R}^6_+$ is relatively compact in $\boldsymbol{F}(\boldsymbol{\Omega})$ with a smooth dynamic phase flow $\phi_t(t_0, \boldsymbol{X})$. Given that $\boldsymbol{\Omega}$ is a closed, convex, and non-empty subset of a Banach space in $\boldsymbol{R}^6_+$, then the couple set of first order differential equation given in (1.3) has a unique solution.

$$\begin{cases} \dot{\boldsymbol{X}}(t) = \boldsymbol{F}(\boldsymbol{X})(t); \quad t \in [0,T] = \boldsymbol{J} \\ \boldsymbol{X}(0) = \boldsymbol{X_0} = (S_0, E_0, A_0, I_0, H_0, R_0) \in \boldsymbol{R}^6_+ \end{cases} \tag{1.3}$$

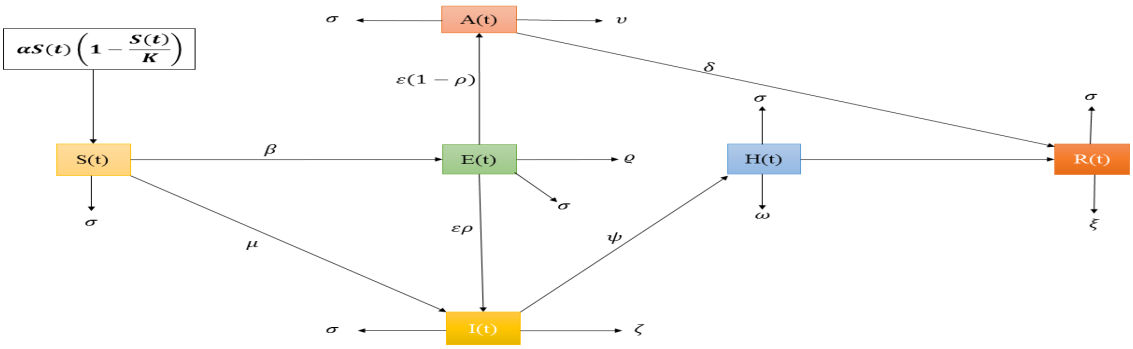

Figure 2: structural model of interaction in population compartments

Remark: Since $\boldsymbol{F} \in C^1$, then $\boldsymbol{F}$ is locally Lipschitz. Theorem 1 guarantees the existence and uniqueness of solution of equations (1.1) and (1.2) with sensitive dependence on initial conditions. The following lemma guides the proof of this theorem.

Lemma 1:[19] If $p, q \geq 1$ is defined with conjugacy $\frac{1}{p} + \frac{1}{q} = 1$, then $\frac{1}{p}x^p + \frac{1}{q}y^q \geq xy \;\; \forall\, x, y \geq 0$.

Lemma 2 (Gronwall's Inequality): Let $u : [0, T] \longrightarrow \boldsymbol{R}$ be continuous and non-negative. Suppose $C \geq 0$ and $K \geq 0$ are such that

$$U(t) \leq C + \int_{t_0}^{t} KU(s)ds \tag{1.4}$$

for all $(t, t_0) \in [0, T]$. Then, for all t in this interval,

$$U(t) \leq Ce^{K(t-t_0)} \tag{1.5}$$

Lemma 3: Suppose $U_k : J \to \boldsymbol{R}^n,\; k = 0, 1, 2, ...,$ is a sequence of continuous functions on a closed interval J such that given $\epsilon > 0$ there is some $N > 0$, and for every $p, q > N$ such that

$$max_{t \in J}|U_p(t) - U_q(t)| < \epsilon \tag{1.6}$$

Then there is a continuous function $U : J \to \boldsymbol{R}^n$ such that

$$max_{t \in J}|U_k(t) - U(t)| \to 0 \;\text{ as }\; k \to \infty \tag{1.7}$$

Moreover, for any t with $|t| \leq h,\;\; U_0(0) < M$

$$\lim_{t \to \infty} \int_0^t U_k(s)ds = \int_0^t U(s)ds \tag{1.8}$$

Remark: This lemma establishes the uniform convergence of any sequence of continuous function using Picard's iteration scheme.

Proof: It suffices to show that the vector-valued functional $\boldsymbol{F}$ is a contractive map. Define two analytic and integral solutions of the considered system in euqation (1.1) and (1.2) as nonlinear continuous functionals $\boldsymbol{X}, \boldsymbol{Y} : \boldsymbol{J} \times \boldsymbol{R}_{+}^{6} \to \boldsymbol{R}$. In closed form, these functions are equivalent solutions to the model defined in equations (1.1) and (1.2) and written as:

$$\begin{aligned} \boldsymbol{X}(t) =& \boldsymbol{X_0} + \int_{t_0}^{t} \boldsymbol{F}(\boldsymbol{X})(\boldsymbol{s})ds \\ \boldsymbol{Y}(t) =& \boldsymbol{Y_0} + \int_{t_0}^{t} \boldsymbol{F}(\boldsymbol{Y})(\boldsymbol{s})ds \end{aligned} \tag{1.9}$$

Geometrically, assume that for all initial solutions that are closed together, any solution that passes through them remains closed for all times, then given $\epsilon^* > 0$ there exist δ^* such that $\|X_0 - Y_0\| < \delta^*$ and

$$|\boldsymbol{X}(\boldsymbol{s}) - \boldsymbol{Y}(\boldsymbol{s})| \leq |\boldsymbol{X_0} - \boldsymbol{Y_0}| + \int_{t_0}^{t} |(\boldsymbol{F}(\boldsymbol{s}), \boldsymbol{X}(\boldsymbol{s})) - \boldsymbol{F}(\boldsymbol{s}, \boldsymbol{Y}(\boldsymbol{s}))|ds \tag{2.0}$$

Apply triangle inequality, and lemma 2 then equation 2.0 yields

$$\begin{cases} \|\boldsymbol{X}(\boldsymbol{s}) - \boldsymbol{Y}(\boldsymbol{s})\| \leq \|\boldsymbol{X_0} - \boldsymbol{Y_0}\| e^{\|\boldsymbol{K}\|h} < \epsilon^*; \quad h \in [0, T], \\ \qquad\qquad \leq \delta^* e^{\|\boldsymbol{K}\|h} < \epsilon^*; \quad h \in [0, T], \\ \|\boldsymbol{K}\| = \max\limits_{1 \leq j \leq 6} \sum\limits_{i=1}^{6} |A_{i,j}|, \quad \rho^*(A_{i,j}) \leq \|A_{i,j}\| \end{cases} \tag{2.1}$$

where ρ^* is the spectral radius of the matrix, $A_{i,j}$. The square matrix $A_{i,j}$, equipped with the norm $\max\limits_{0 \leq i \leq 6} (\|\boldsymbol{X_i}\|, \|\boldsymbol{Y_i}\|) \leq \phi$ is define as follows,

$$\begin{bmatrix} (\alpha + \frac{2\alpha\phi}{K} + \phi(\beta + \mu) + \sigma) & \beta\phi & \mu\phi & 0 & 0 & 0 \\ \beta\phi & \beta\phi + \epsilon(\rho - 1) + (\varrho + \sigma) & 0 & 0 & 0 & 0 \\ \mu\phi & \epsilon\rho & \mu\phi + \psi + \zeta + \sigma & 0 & 0 & 0 \\ 0 & (\epsilon\rho - 1) & 0 & \delta + \nu + \sigma & 0 & 0 \\ 0 & 0 & \psi & 0 & \eta + \omega + \sigma & 0 \\ 0 & 0 & 0 & 0 & 0 & \xi + \sigma \end{bmatrix}$$

By choosing $\delta^* = \frac{\epsilon^*}{e^{\|\boldsymbol{K}\|h}}$, the operator $\boldsymbol{F}$ on $\boldsymbol{X}, \boldsymbol{Y}$ is a contractive map. Using Lemma 3 for identical initial conditions, say $\|\boldsymbol{X_0} - \boldsymbol{Y_0}\| = 0$, then $\boldsymbol{X}(\boldsymbol{s}) = \boldsymbol{Y}(\boldsymbol{s})$. Hence the proof is complete.

Corollary: *In this model, systems (1.1) and (1.2) are ultimately bounded in the positive invariant region of* $\boldsymbol{\Omega} \subset \mathbb{R}_{+}^{6}$ *if* $\frac{\epsilon^*}{exp(\|K\|h)} < 1$.

Remark: This theorem establishes the analytic solution of equations (1.1) and (1.2), using the fundamental theory of functional analysis. Since uniformly a continuous function is ultimately bounded.

2.0 Dynamics at Equilibrium Points in COVID-19 Model

2.1 Existence of Positive Equilibrium Points in the Model:

The steady state behaviour of the model defines the disease free equilibrium(E_0), and endemic equilibrium (E_1) points of the model given in equation (2.2)

$$
\begin{cases}
E_0^* &= \left(S_0^* = \frac{\kappa\,(\alpha-\sigma)}{\alpha}, E_0^* = 0, I_0^* = 0, A_0^* = 0, H_0^* = 0, R_0^* = 0\right)\ E_1^* = \left(S_1^*, E_1^*, I_1^*, A_1^*, H_1^*, R_1^* = \frac{P^*}{Q^*}\right) \\
S_1^* &= \left(\frac{\rho\epsilon+\sigma+\varrho-\epsilon}{\beta}\right),\ E_1^* = \frac{(-\mu\,\rho\,\varepsilon+\beta\,\psi+\beta\,\sigma+\beta\,\varsigma-\mu\,\sigma-\mu\,\varrho+\mu\,\varepsilon)(\alpha\,\beta\,\kappa-\alpha\,\rho\,\varepsilon-\beta\,\kappa\,\sigma-\alpha\,\sigma-\alpha\,\varrho+\alpha\,\varepsilon)}{\beta^2\kappa\,(\beta\,\psi+\beta\,\sigma+\beta\,\varsigma-\mu\,\sigma-\mu\,\varrho+\mu\,\varepsilon)} \\
A_1^* &= \frac{\varepsilon\,(\alpha\,\beta\,\kappa-\alpha\,\rho\,\varepsilon-\beta\,\kappa\,\sigma-\alpha\,\sigma-\alpha\,\varrho+\alpha\,\varepsilon)\left(-\mu\,\rho^2\varepsilon+\beta\,\psi\,\rho+\beta\,\rho\,\sigma+\beta\,\rho\,\varsigma-\mu\,\rho\,\sigma-\mu\,\rho\,\varrho+2\,\mu\,\rho\,\varepsilon-\beta\,\psi-\beta\,\sigma-\beta\,\varsigma+\mu\,\sigma+\mu\,\varrho-\mu\,\varepsilon\right)}{\beta^2\kappa(\sigma+\delta+\upsilon)(\beta\,\psi+\beta\,\sigma+\beta\,\varsigma-\mu\,\sigma-\mu\,\varrho+\mu\,\varepsilon)}, \\
I_1^* &= \frac{(\alpha\,\beta\,\kappa-\alpha\,\rho\,\varepsilon-\beta\,\kappa\,\sigma-\alpha\,\sigma-\alpha\,\varrho+\alpha\,\varepsilon)\varepsilon\,\rho}{(\beta\,\psi+\beta\,\sigma+\beta\,\varsigma-\mu\,\sigma-\mu\,\varrho+\mu\,\varepsilon)\beta\,\kappa} \\
H_1^* &= \frac{\psi\,\rho\,\varepsilon\,(\alpha\,\beta\,\kappa-\alpha\,\rho\,\varepsilon-\beta\,\kappa\,\sigma-\alpha\,\sigma-\alpha\,\varrho+\alpha\,\varepsilon)}{\beta\,\kappa\left(\beta\,\eta\,\psi+\beta\,\eta\,\sigma+\beta\,\eta\,\varsigma+\beta\,\omega\,\psi+\beta\,\omega\,\sigma+\beta\,\omega\,\varsigma+\beta\,\psi\,\sigma+\beta\,\sigma^2+\beta\,\sigma\,\varsigma-\eta\,\mu\,\sigma-\eta\,\mu\,\varrho+\eta\,\mu\,\varepsilon-\mu\,\omega\,\sigma-\mu\,\omega\,\varrho+\mu\,\omega\,\varepsilon-\mu\,\sigma^2-\mu\,\sigma\,\varrho+\mu\,\sigma\,\varepsilon\right)} \\
P^* &= \varepsilon(-\delta\,\eta\,\mu\,\rho^2\varepsilon - \delta\,\mu\,\omega\,\rho^2\varepsilon - \delta\,\mu\,\rho^2\sigma\,\varepsilon + 2\,\beta\,\delta\,\eta\,\psi\,\rho + \beta\,\delta\,\eta\,\rho\,\sigma + \beta\,\delta\,\eta\,\rho\,\varsigma + \beta\,\delta\,\omega\,\psi\,\rho + \\
&\quad \beta\,\delta\,\omega\,\rho\,\sigma + \beta\,\delta\,\omega\,\rho\,\varsigma + \beta\,\delta\,\psi\,\rho\,\sigma + \beta\,\delta\,\rho\,\sigma^2 + \beta\,\delta\,\rho\,\sigma\,\varsigma + \beta\,\eta\,\psi\,\rho\,\sigma + \beta\,\eta\,\psi\,\rho\,\upsilon - \delta\,\eta\,\mu\,\rho\,\sigma - \\
&\quad \delta\,\eta\,\mu\,\rho\,\varrho + 2\,\delta\,\eta\,\mu\,\rho\,\varepsilon - \delta\,\mu\,\omega\,\rho\,\sigma - \delta\,\mu\,\omega\,\rho\,\varrho + 2\,\delta\,\mu\,\omega\,\rho\,\varepsilon - \delta\,\mu\,\rho\,\sigma^2 - \delta\,\mu\,\rho\,\sigma\,\varrho + 2\,\delta\,\mu\,\rho\,\sigma\,\varepsilon - \\
&\quad \beta\,\delta\,\eta\,\psi - \beta\,\delta\,\eta\,\sigma - \beta\,\delta\,\eta\,\varsigma - \beta\,\delta\,\omega\,\psi - \beta\,\delta\,\omega\,\sigma - \beta\,\delta\,\omega\,\varsigma - \beta\,\delta\,\psi\,\sigma - \beta\,\delta\,\sigma^2 - \beta\,\delta\,\sigma\,\varsigma + \\
&\quad \delta\,\eta\,\mu\,\sigma + \delta\,\eta\,\mu\,\varrho - \delta\,\eta\,\mu\,\varepsilon + \delta\,\mu\,\omega\,\sigma + \delta\,\mu\,\omega\,\varrho - \delta\,\mu\,\omega\,\varepsilon + \delta\,\mu\,\sigma^2 + \delta\,\mu\,\sigma\,\varrho - \delta\,\mu\,\sigma\,\varepsilon) \\
&\quad (\alpha\,\beta\,\kappa - \alpha\,\rho\,\varepsilon - \beta\,\kappa\,\sigma - \alpha\,\sigma - \alpha\,\varrho + \alpha\,\varepsilon) \\
Q^* &= \beta^2\kappa(\beta\,\eta\,\psi + \beta\,\eta\,\sigma + \beta\,\eta\,\varsigma + \beta\,\omega\,\psi + \beta\,\omega\,\sigma + \beta\,\omega\,\varsigma + \beta\,\psi\,\sigma + \beta\,\sigma^2 + \beta\,\sigma\,\varsigma - \eta\,\mu\,\sigma - \eta\,\mu\,\varrho + \\
&\quad \eta\,\mu\,\varepsilon - \mu\,\omega\,\sigma - \mu\,\omega\,\varrho + \mu\,\omega\,\varepsilon - \mu\,\sigma^2 - \mu\,\sigma\,\varrho + \mu\,\sigma\,\varepsilon)
\end{cases}
\tag{2.2}
$$

2.2 Basic Reproduction Number(R_0) of COVID-19

The basic reproduction number (R_0) is a dimensionless parameter that determines an average spread of the disease by an infectious person during contact with the susceptible, exposed, asymptomatic and hospitalized populations. The expected spreading parameter quantifies continuous spread for infection if $R_0 > 1$, and extinction of the spread if $R_0 < 1$ near the disease free equilibrium point in the model. In this model the sub-populations that are responsible for spreading the disease are exposed, $E(t)$; infected $E(t)$; asymptomatic, $A(t)$; and hospitalized, $H(t)$ classes. Using the Next Generation Operator[20] at the disease free equilibrium (E_0) in system (2.2) , a compartmental subsystem of transmission and transfer matrices (F, V) are obtained as follows. In this case, the basic reproduction number (R_0) is the spectral radius of the matrix operator; FV^{-1}

$$
\begin{cases}
F = & \begin{bmatrix} \frac{\beta\kappa\,(\alpha-\sigma)}{\alpha} & 0 & 0 & 0 \\ 0 & \frac{\mu\,\kappa\,(\alpha-\sigma)}{\alpha} & 0 & 0 \\ 0 & 0 & 0 & 0 \\ 0 & 0 & 0 & 0 \end{bmatrix} \\
V = & \begin{bmatrix} \varrho+\sigma+\varepsilon\,(\rho-1) & 0 & 0 & 0 \\ -\varepsilon\,\rho & \psi+\sigma+\varsigma & 0 & 0 \\ -\varepsilon\,(\rho-1) & 0 & \delta+\upsilon+\sigma & 0 \\ 0 & -\psi & 0 & \eta+\omega+\sigma \end{bmatrix} \\
V^{-1} = & \begin{bmatrix} (\varepsilon\,\rho+\sigma+\varrho-\varepsilon)^{-1} & 0 & 0 & 0 \\ \frac{\varepsilon\,\rho}{(\varepsilon\,\rho+\sigma+\varrho-\varepsilon)(\psi+\sigma+\varsigma)} & (\psi+\sigma+\varsigma)^{-1} & 0 & 0 \\ \frac{\varepsilon\,(\rho-1)}{(\varepsilon\,\rho+\sigma+\varrho-\varepsilon)(\delta+\upsilon+\sigma)} & 0 & (\delta+\upsilon+\sigma)^{-1} & 0 \\ \frac{\psi\,\varepsilon\,\rho}{(\varepsilon\,\rho+\sigma+\varrho-\varepsilon)(\psi+\sigma+\varsigma)(\eta+\omega+\sigma)} & \frac{\psi}{(\psi+\sigma+\varsigma)(\eta+\omega+\sigma)} & 0 & (\eta+\omega+\sigma)^{-1} \end{bmatrix} \\
P(FV^{-1},\lambda) = & \lambda^4 - \frac{\kappa\,(\alpha-\sigma)(\mu\,\rho\,\varepsilon+\beta\,\psi+\beta\,\sigma+\beta\,\varsigma+\mu\,\sigma+\mu\,\varrho-\mu\,\varepsilon)\lambda^3}{\alpha\,(\varepsilon\,\rho+\sigma+\varrho-\varepsilon)(\psi+\sigma+\varsigma)} + \frac{\mu\,\kappa^2(\alpha-\sigma)^2\beta\,\lambda^2}{\alpha^2(\psi+\sigma+\varsigma)(\varepsilon\,\rho+\sigma+\varrho-\varepsilon)},\ \lambda_1 = \frac{\mu\,\kappa\,(\alpha-\sigma)}{\alpha\,(\psi+\sigma+\varsigma)}, \\
& \lambda_2 = \frac{\beta\,\kappa\,(\alpha-\sigma)}{\alpha\,(\varepsilon\,\rho+\sigma+\varrho-\varepsilon)} \\
R_0 = \rho(FV^{-1}) = & \max(\lambda_1,\lambda_2) = \frac{\beta\,\kappa\,(\alpha-\sigma)}{\alpha\,(\varepsilon\,\rho+\sigma+\varrho-\varepsilon)}
\end{cases}
\tag{2.3}
$$

Lemma 4[21]Let $A \in \mathbb{R}^{n\times n}$ be a real matrix, with $P(\lambda) = \det|\lambda I - A| = a_0\lambda^n + a_1\lambda^{n-1} + \cdots + a_{n-1}\lambda + a_n = 0$. If $a_i > 0 (i = 1, 2, \ldots, n)$, then $P(\lambda)$ is Hurwitzian if and only if

$$\begin{cases} \Delta_1 = a_1 > 0,\ \Delta_2 = \begin{vmatrix} a_1 & a_0 \\ a_3 & a_2 \end{vmatrix} > 0, \Delta_3 = \begin{vmatrix} a_1 & a_0 & 0 \\ a_3 & a_2 & a_1 \\ a_5 & a_4 & a_3 \end{vmatrix} > 0, \\ \Delta_n = \begin{vmatrix} a_1 & a_0 & 0 & 0 & 0 & \cdots & 0 & 0 & 0 & 0 \\ a_3 & a_2 & a_1 & 0 & 0 & 0 & \cdots & 0 & 0 & 0 \\ a_5 & a_4 & a_3 & a_2 & a_1 & 0 & 0 & \cdots & 0 & 0 \\ \cdots & \cdots & & & & & & & \cdots & \cdots \\ \cdots & \cdots & & & & & & & a_{n-1} & a_{n-2} \\ a_{2n-1} & a_{2n-2} & \cdots & \cdots & \cdots & \cdots & \cdots & \cdots & \cdots & a_n \end{vmatrix} = \Delta_{n-1}a_n > 0, \end{cases} \tag{2.4}$$

where $a_s = 0\ \forall\ s < 0$ or $s > n$.

Lemma 5 (Descarte's Rule of Sign)[21]: Consider the sequence of coefficient of real polynomial $P_n(\lambda) = a_n\lambda^n + a_{n-1}\lambda^{n-1} + \cdots + a_1\lambda + a_0$ defined as $\{a_n\}_{i=0}^{i=n}$. Let k be the total number of sign changes from one coefficient to the next in the sequence, then the number of positive roots of the polynomial is either equal to k or $k - 2m$, where m is an even integer. (Note, if $k = 1$, then there is exactly one positive real root).

Theorem 2: The disease free equilibrium point E_0 of equation (1.2) is locally asymptotically stable if $R_0 < 1$, and unstable if $R_0 > 1$.

Proof

The Jacobian matrix of the model (1.2) and (1.2), evaluated at the disease free equilibrium yielded a characteristic polynomial and corresponding eigenvalues as given in (2.5)

$$\begin{cases} P(\lambda) = & \lambda^6 - (J_{11}J_{22}J_{33}J_{44}J_{55}J_{66})\lambda^5 + (J_{11}J_{22} + J_{11}J_{33} + J_{11}J_{44} + J_{11}J_{55} + J_{11}J_{66} + J_{33}J_{22} \\ & +J_{44}J_{22} + J_{55}J_{22} + J_{66}J_{22} + J_{33}J_{44} + J_{33}J_{55} + J_{33}J_{66} + J_{55}J_{44} + J_{66}J_{44} + J_{55}J_{66} \\ & -J_{56}J_{65})\lambda^4 + (-J_{11}J_{22}J_{33} - J_{11}J_{22}J_{44} - J_{11}J_{22}J_{55} - J_{11}J_{22}J_{55} - J_{11}J_{33}J_{44} - J_{11}J_{33}J_{55} \\ & -J_{11}J_{33}J_{66} - J_{11}J_{44}J_{55} - J_{11}J_{44}J_{66} - J_{11}J_{55}J_{66} + J_{11}J_{56}J_{65} - J_{22}J_{33}J_{44} - J_{22}J_{33}J_{55} \\ & J_{22}J_{33}J_{66} - J_{22}J_{55}J_{44} - J_{22}J_{66}J_{44} - J_{22}J_{55}J_{66} + J_{22}J_{56}J_{65} - J_{33}J_{44}J_{55} - J_{33}J_{44}J_{66} \\ & -J_{33}J_{55}J_{66} + J_{33}J_{56}J_{65} - J_{44}J_{55}J_{66} + J_{44}J_{56}J_{65})\lambda^3 + (J_{11}J_{22}J_{33}J_{44} + J_{11}J_{22}J_{33}J_{55} \\ & J_{11}J_{22}J_{33}J_{66} + J_{11}J_{22}J_{44}J_{55} + J_{11}J_{22}J_{44}J_{66} + J_{11}J_{22}J_{55}J_{66} - J_{11}J_{22}J_{56}J_{65} \\ & +J_{11}J_{33}J_{44}J_{55} - J_{11}J_{66}J_{33}J_{44} - J_{11}J_{44}J_{56}J_{65} + J_{22}J_{33}J_{44}J_{55} + J_{22}J_{33}J_{44}J_{66} \\ & -J_{22}J_{33}J_{56}J_{65} + J_{22}J_{44}J_{55}J_{66} - J_{22}J_{44}J_{56}J_{65} + J_{33}J_{44}J_{55}J_{66} - J_{33}J_{44}J_{56}J_{65})\lambda^2 + \\ & (-J_{11}J_{22}J_{33}J_{44}J_{55} - J_{11}J_{22}J_{33}J_{44}J_{66} - J_{11}J_{22}J_{33}J_{66}J_{55} + J_{11}J_{22}J_{33}J_{56}J_{65} \\ & -J_{11}J_{22}J_{44}J_{66}J_{55} + J_{11}J_{22}J_{44}J_{56}J_{65} - J_{11}J_{33}J_{44}J_{55}J_{66} + J_{22}J_{33}J_{44}J_{56}J_{65})\lambda \\ & +J_{11}J_{22}J_{33}J_{44}J_{55}J_{66} - J_{11}J_{22}J_{33}J_{44}J_{56}J_{65} \\ and & \\ & \lambda_1 = -\xi - \sigma\ , \lambda_2 = -\alpha + \sigma\ , \lambda_3 = \frac{\alpha\,\kappa\,\mu - \mu\,\kappa\,\sigma - \alpha\,\psi - \alpha\,\sigma - \alpha\,\varsigma}{\alpha}\ , \lambda_4 = -\eta - \omega - \sigma\ , \\ & \lambda_5 = -\delta - \sigma - \upsilon\ , \lambda_6 = \frac{\alpha\,\beta\,\kappa - \alpha\,\rho\,\varepsilon - \beta\,\kappa\,\sigma - \alpha\,\sigma - \alpha\,\varrho + \alpha\,\varepsilon}{\alpha} \end{cases} \tag{2.5}$$

using the matrix

$$J_{ij}(E_0) = \begin{bmatrix} -\alpha+\sigma & -\frac{\beta\,\kappa\,(\alpha-\sigma)}{\alpha} & -\frac{\mu\,\kappa\,(\alpha-\sigma)}{\alpha} & 0 & 0 & 0 \\ 0 & \frac{\alpha(-\varrho-\sigma-\varepsilon\,(\rho-1)+\beta\,\kappa\,)(\alpha-\sigma)}{\alpha} & 0 & 0 & 0 & 0 \\ 0 & \varepsilon\,\rho & \frac{\mu\,\kappa\,(\alpha-\sigma)}{\alpha}-\psi-\sigma-\varsigma & 0 & 0 & 0 \\ 0 & \varepsilon\,(\rho-1) & 0 & -\delta-\sigma-\upsilon & 0 & 0 \\ 0 & 0 & \psi & 0 & -\eta-\omega-\sigma & 0 \\ 0 & 0 & 0 & \delta & \eta & -\xi-\sigma \end{bmatrix}$$

Then, ensuring that all eigenvalues identified in 2.5 are negatives; $(\alpha > \sigma, \lambda_{i\ (i=1,2,\ldots 6)} < 0)$ guarantees $R_0 = \frac{\beta\,\kappa\,(\alpha-\sigma)}{\alpha\,(\varepsilon\,\rho+\sigma+\varrho-\varepsilon)} < 1$ or otherwise and the proof is complete.

Theorem 3: The endemic equilibrium point (E_1) defined in 2.2 is locally asymptotically stable for $R_0 > 1$

Proof Assume that the basic reproduction number $R_0 > 1$, then the endemic equilibrium point exists. Evaluating the Jacobian matrix of (1.2) at the endemic equilibrium (E_1) point yields:

$$\begin{cases} J_{ij}(E_1) = \begin{bmatrix} -\frac{\alpha\,(\varepsilon(\rho-1)+\sigma+\varrho)}{\beta\kappa} & -\rho\varepsilon-\sigma-\varrho+\varepsilon & -\frac{(\varepsilon(\rho-1)+\sigma+\varrho)\mu}{\beta} & 0 & 0 & 0 \\ J_{21} & 0 & 0 & 0 & 0 & 0 \\ J_{31} & \rho\varepsilon & J_{33} & 0 & 0 & 0 \\ 0 & \varepsilon\,(\rho-1) & 0 & -\delta-\sigma-\upsilon & 0 & 0 \\ 0 & 0 & \psi & 0 & -\eta-\omega-\sigma & 0 \\ 0 & 0 & 0 & \delta & \eta & -\xi-\sigma \end{bmatrix} \\ J_{21} = \frac{(-\beta\kappa(\alpha-\sigma)+\alpha(\varepsilon(\rho-1)+\sigma+\varrho))((-\psi-\sigma-\varsigma)\beta+(\varepsilon(\rho-1)+\sigma+\varrho)\mu)}{\beta\kappa((\psi+\sigma+\varsigma)\beta+\mu(-\sigma-\varrho+\varepsilon))}, \quad J_{31} = -\frac{(-\beta\kappa(\alpha-\sigma)+\alpha(\varepsilon(\rho-1)+\sigma+\varrho))\rho\,\varepsilon\mu}{\beta\kappa((\psi+\sigma+\varsigma)\beta+\mu(-\sigma-\varrho+\varepsilon))}, \\ J_{33} = \frac{(-\psi-\sigma-\varsigma)\beta+(\varepsilon(\rho-1)+\sigma+\varrho)\mu}{\beta}, \ \forall\, i,j\ 1,2,\ldots,6 \end{cases} \tag{2.6}$$

Using the entries of the Jacobian matrix in system 2.6, to construct the corresponding characteristic polynomial 2.7 at the endemic equilibrium point, and applying lemma 4 yields the required result as follows. Recall that lemma 4 guarantees the existence of negative roots of the given polynomial in equation (2.7)

$$\begin{cases} P(\lambda) = & \lambda^6 + (-J_{66}-J_{55}-J_{44}-J_{33}-J_{11})\,\lambda^5 + (J_{11}\,J_{33}+J_{11}\,J_{44}+J_{11}\,J_{55}+J_{11}\,J_{66}-J_{12}\,J_{21} \\ & -J_{13}\,J_{31}+J_{33}\,J_{44}+J_{33}\,J_{55}+J_{33}\,J_{66}+J_{44}\,J_{55}+J_{44}\,J_{66}+J_{55}\,J_{66})\lambda^4 + (-J_{11}\,J_{33}\,J_{44} \\ & -J_{11}\,J_{33}\,J_{55}-J_{11}\,J_{33}\,J_{66}-J_{11}\,J_{44}\,J_{55}-J_{11}\,J_{44}\,J_{66}-J_{11}\,J_{55}\,J_{66}+J_{12}\,J_{21}\,J_{33}+ \\ & J_{12}\,J_{21}\,J_{44}+J_{12}\,J_{21}\,J_{55}+J_{12}\,J_{21}\,J_{66}-J_{13}\,J_{21}\,J_{32}+J_{13}\,J_{31}\,J_{44}+J_{13}\,J_{31}\,J_{55}+ \\ & J_{13}\,J_{31}\,J_{66}-J_{33}\,J_{44}\,J_{55}-J_{33}\,J_{44}\,J_{66}-J_{33}\,J_{55}\,J_{66}-J-44\,J_{55}\,J_{66})\lambda^3 + (J_{11}\,J_{33}\,J_{44}\,J_{55} \\ & +J_{11}\,J_{33}\,J_{44}\,J_{66}+J_{11}\,J_{33}\,J_{55}\,J_{66}+J_{11}\,J_{44}\,J_{55}\,J_{66}-J_{12}\,J_{21}\,J_{33}\,J_{44}-J_{12}\,J_{21}\,J_{33}\,J_{55}- \\ & J_{12}\,J_{21}\,J_{33}\,J_{66}-J_{12}\,J_{21}\,J_{44}\,J_{55}-J_{12}\,J_{21}\,J_{44}\,J_{66}-J_{12}\,J_{21}\,J_{55}\,J_{66}+J_{13}\,J_{21}\,J_{32}\,J_{44}+ \\ & J_{13}\,J_{21}\,J_{32}\,J_{55}+J_{13}\,J_{21}\,J_{32}\,J_{66}-J_{13}\,J_{31}\,J_{44}\,J_{55}-J_{13}\,J_{31}\,J_{44}\,J_{66}-J_{13}\,J_{31}\,J_{55}\,J_{66}+ \\ & J_{33}\,J_{44}\,J_{55}\,J_{66})\lambda^2 + (-J_{11}\,J_{33}\,J_{44}\,J_{55}\,J_{66}+J_{12}\,J_{21}\,J_{33}\,J_{44}\,J_{55}+J_{12}\,J_{21}\,J_{33}\,J_{44}\,J_{66}+ \\ & J_{12}\,J_{21}\,J_{33}\,J_{55}\,J_{66}+J_{12}\,J_{21}\,J_{44}\,J_{55}\,J_{66}-J_{13}\,J_{21}\,J_{32}\,J_{44}\,J_{55}-J_{13}\,J_{21}\,J_{32}\,J_{44}\,J_{66}- \\ & J_{13}\,J_{21}\,J_{32}\,J_{55}\,J_{66}+J_{13}\,J_{31}\,J_{44}\,J_{55}\,J_{66})\lambda - J_{66}\,J_{55}\,J_{44}\,J_{21}\,(J_{12}\,J_{33}-J_{13}\,J_{32}) \end{cases} \tag{2.7}$$

3.0 Bifurcation and Hysteresis Effects of COVID-19 Model

In this section, a center manifold theory is applied to unfold the bifurcation behaviour of the model in system (1.2) around the disease free equilibrium E_0 and endemic equilibrium point E_1. This established the local stability of a

non-hyperbolic equilibrium emanated from the centre manifold, and existence of another equilibrium, bifurcated from the non-hyperbolic equilibrium.

3.1 Centre Manifold Dynamics in COVID-19 Model

Theorem 4[[22]] Consider a general system of ordinary differential equation with parameter ϕ in closed form as:

$$\frac{dX}{dt} = F(X, \phi),\ F : R^n \times R \to R \ \ and \ \ F \in C^2(R^n \times R) \tag{2.8}$$

WLG, it is assumed that 0 is an equilibrium point of the system (2.8) for all values of the parameter ϕ such that $F(0, \phi) = 0$. Similarly, assume that

- $A = D_X F_i(0,0) = \left(\frac{\partial F}{\partial X_i}\right)(0,0)$ is the linearization matrix of system 2.8 around the equilibrium 0 with *phi* evaluated at 0. Zero being the simple eigenvalue of the matrix A, and all other eigenvalues of A have negative real parts.
- Matrix A has a non-negative right eigenvector w and a left eigenvector v corresponding to the eigenvalue. Let F_k be the kth component of F and

$$\begin{cases} a = \sum\limits_{k,i,j=1}^{n} v_k w_i w_j \left(\frac{\partial^2 F_k}{\partial X_i \partial X_j}\right)(0,0) \\ b = \sum\limits_{k,i,j=1}^{n} v_k w_i \left(\frac{\partial^2 F_k}{\partial X_i \partial \phi}\right)(0,0) \end{cases} \tag{2.9}$$

The local dynamics of system 2.8 around zero(0) are totally determined by the numerical values of parameters a and b as follows:

i $a > 0, b > 0$. When $\phi < 0$ with $|\phi \ll 1|$, 0 is locally asymptotically stable, and there exists a positive unstable equilibrium; when $0 < \phi \ll 1$, 0 is unstable and there exists a negative and locally asymptotically stable equilibrium.

ii $a < 0, b > 0$. When $\phi < 0$ with $|\phi \ll 1|$, 0 is unstable; when $0 < \phi \ll 1$, 0 is locally asymptotically stable, and positive unstable equilibrium appears.

iii $a > 0, b < 0$. When $\phi < 0$ with $|\phi \ll 1|$, 0 is unstable, and there exists a locally asymptotically stable negative equilibrium; when $0 < \phi \ll 1$, 0 is locally asymptotically stable, and positive unstable equilibrium appears.

iv $a < 0, b > 0$. When ϕ changes from negative to positive, 0 changes its stability from stable to unstable. Correspondingly a negative equilibrium becomes positive and locally asymptotically stable.

Remark When $a < 0, b > 0$, the bifurcation at $\phi = 0$ is transcritical(forward) bifurcation with possible hysteresis effect.

3.2 Eigenvalue and Eigenvector Analysis at the Centre Manifold

Theorem 4 can be applied to model of system 1.2 be taking the state variable as components of vector $X_i = (S, E, I, A, H, R)^T \approxeq (x_1, x_2, x_3, x_4, x_5, x_6)^T$. In this model the quasi-lockdown parameter κ, which controls the influx of susceptible class to transmission and transition of the infection in the entire population is the bifurcation parameter. This lockdown parameter begins to control the dynamics of the model as the disease start spreading, more or less when the basic reproduction number $R_0 \leq 1$. This dynamics can be visualized when evaluating the

Jacobian matrix in system 2.5 at the disease free equilibrium point E_0. In this case the bifurcation parameter κ yields a simple zero eigenvalue and the corresponding right and left eigenvectors defined as follows.

$$
\begin{cases}
 & R_0 = 1, \kappa^* = \frac{\rho\varepsilon+\sigma+\varrho-\varepsilon}{\beta(\alpha-\sigma)} \\
 & w = \left[w_1 = \frac{a_1}{a_2}\ \ w_2 = \frac{b_1}{b_2}\ \ w_3 = \frac{c_1}{c_2}\ \ w_4 = \frac{d_1}{d_2}\ \ w_5 = \frac{c_1}{c_2},\ \ w_6 = 1\right]^T \\
 & v = [v_1 = 0\ v_2 = 1\ v_3 = 0\ v_4 = 0\ v_5 = 0\ v_6 = 0]^T \\
where & \\
a_1 = & -(\rho\,\varepsilon+\sigma+\varrho-\varepsilon)\,(\delta+\sigma+\upsilon)\ (\eta+\omega+\sigma)\,(\xi+\sigma)\,(\beta\,\psi+\beta\,\sigma+\beta\,\varsigma-\mu\,\sigma-\mu\,\varrho+\mu\,\varepsilon) \\
a_2 = & (-\delta\,\eta\,\mu\,\rho^2\varepsilon-\delta\,\mu\,\omega\,\rho^2\varepsilon-\delta\,\mu\,\rho^2\sigma\,\varepsilon+2\,\beta\,\delta\,\eta\,\psi\,\rho+\beta\,\delta\,\eta\,\rho\,\sigma+\beta\,\delta\,\eta\,\rho\,\varsigma+\beta\,\delta\,\omega\,\psi\,\rho+\beta\,\delta\,\omega\,\rho\,\sigma \\
 & +\beta\,\delta\,\omega\,\rho\,\varsigma+\beta\,\delta\,\psi\,\rho\,\sigma+\beta\,\delta\,\rho\,\sigma^2+\beta\,\delta\,\rho\,\sigma\,\varsigma+\beta\,\eta\,\psi\,\rho\,\sigma+\beta\,\eta\,\psi\,\rho\,\upsilon-\delta\,\eta\,\mu\,\rho\,\sigma-\delta\,\eta\,\mu\,\rho\,\varrho \\
 & +2\,\delta\,\eta\,\mu\,\rho\,\varepsilon-\delta\,\mu\,\omega\,\rho\,\sigma-\delta\,\mu\,\omega\,\rho\,\varrho+2\,\delta\,\mu\,\omega\,\rho\,\varepsilon-\delta\,\mu\,\rho\,\sigma^2-\delta\,\mu\,\rho\,\sigma\,\varrho+2\,\delta\,\mu\,\rho\,\sigma\,\varepsilon-\beta\,\delta\,\eta\,\psi \\
 & -\beta\,\delta\,\eta\,\sigma-\beta\,\delta\,\eta\,\varsigma-\beta\,\delta\,\omega\,\psi-\beta\,\delta\,\omega\,\sigma-\beta\,\delta\,\omega\,\varsigma-\beta\,\delta\,\psi\,\sigma-\beta\,\delta\,\sigma^2-\beta\,\delta\,\sigma\,\varsigma+\delta\,\eta\,\mu\,\sigma+ \\
 & \delta\,\eta\,\mu\,\varrho-\delta\,\eta\,\mu\,\varepsilon+\delta\,\mu\,\omega\,\sigma+\delta\,\mu\,\omega\,\varrho-\delta\,\mu\,\omega\,\varepsilon+\delta\,\mu\,\sigma^2+\delta\,\mu\,\sigma\,\varrho-\delta\,\mu\,\sigma\,\varepsilon)\varepsilon\ (\alpha-\sigma) \\
b_1 = & (-\mu\,\rho\,\varepsilon+\beta\,\psi+\beta\,\sigma+\beta\,\varsigma-\mu\,\sigma-\mu\,\varrho+\mu\,\varepsilon)\,(\delta+\sigma+\upsilon)\,(\eta+\omega+\sigma)\,(\xi+\sigma) \\
b_2 = & (-\delta\,\eta\,\mu\,\rho^2\varepsilon-\delta\,\mu\,\omega\,\rho^2\varepsilon-\delta\,\mu\,\rho^2\sigma\,\varepsilon+2\,\beta\,\delta\,\eta\,\psi\,\rho+\beta\,\delta\,\eta\,\rho\,\sigma+\beta\,\delta\,\eta\,\rho\,\varsigma+\beta\,\delta\,\omega\,\psi\,\rho+\beta\,\delta\,\omega\,\rho\,\sigma \\
 & +\beta\,\delta\,\omega\,\rho\,\varsigma+\beta\,\delta\,\psi\,\rho\,\sigma+\beta\,\delta\,\rho\,\sigma^2+\beta\,\delta\,\rho\,\sigma\,\varsigma+\beta\,\eta\,\psi\,\rho\,\sigma+\beta\,\eta\,\psi\,\rho\,\upsilon-\delta\,\eta\,\mu\,\rho\,\sigma-\delta\,\eta\,\mu\,\rho\,\varrho \\
 & +2\,\delta\,\eta\,\mu\,\rho\,\varepsilon-\delta\,\mu\,\omega\,\rho\,\sigma-\delta\,\mu\,\omega\,\rho\,\varrho+2\,\delta\,\mu\,\omega\,\rho\,\varepsilon-\delta\,\mu\,\rho\,\sigma^2-\delta\,\mu\,\rho\,\sigma\,\varrho+2\,\delta\,\mu\,\rho\,\sigma\,\varepsilon-\beta\,\delta\,\eta\,\psi \\
 & -\beta\,\delta\,\eta\,\sigma-\beta\,\delta\,\eta\,\varsigma-\beta\,\delta\,\omega\,\psi-\beta\,\delta\,\omega\,\sigma-\beta\,\delta\,\omega\,\varsigma-\beta\,\delta\,\psi\,\sigma-\beta\,\delta\,\sigma^2-\beta\,\delta\,\sigma\,\varsigma+\delta\,\eta\,\mu\,\sigma+ \\
 & \delta\,\eta\,\mu\,\varrho-\delta\,\eta\,\mu\,\varepsilon+\delta\,\mu\,\omega\,\sigma+\delta\,\mu\,\omega\,\varrho-\delta\,\mu\,\omega\,\varepsilon+\delta\,\mu\,\sigma^2+\delta\,\mu\,\sigma\,\varrho-\delta\,\mu\,\sigma\,\varepsilon)\varepsilon \\
c_1 = & \beta\rho(\delta+\sigma+\nu)(\eta+\omega+\sigma)(\xi+\sigma) \\
c_2 = & (-\delta\,\eta\,\mu\,\rho^2\varepsilon-\delta\,\mu\,\omega\,\rho^2\varepsilon-\delta\,\mu\,\rho^2\sigma\,\varepsilon+2\,\beta\,\delta\,\eta\,\psi\,\rho+\beta\,\delta\,\eta\,\rho\,\sigma+\beta\,\delta\,\eta\,\rho\,\varsigma+\beta\,\delta\,\omega\,\psi\,\rho+\beta\,\delta\,\omega\,\rho\,\sigma \\
 & +\beta\,\delta\,\omega\,\rho\,\varsigma+\beta\,\delta\,\psi\,\rho\,\sigma+\beta\,\delta\,\rho\,\sigma^2+\beta\,\delta\,\rho\,\sigma\,\varsigma+\beta\,\eta\,\psi\,\rho\,\sigma+\beta\,\eta\,\psi\,\rho\,\upsilon-\delta\,\eta\,\mu\,\rho\,\sigma-\delta\,\eta\,\mu\,\rho\,\varrho \\
 & +2\,\delta\,\eta\,\mu\,\rho\,\varepsilon-\delta\,\mu\,\omega\,\rho\,\sigma-\delta\,\mu\,\omega\,\rho\,\varrho+2\,\delta\,\mu\,\omega\,\rho\,\varepsilon-\delta\,\mu\,\rho\,\sigma^2-\delta\,\mu\,\rho\,\sigma\,\varrho+2\,\delta\,\mu\,\rho\,\sigma\,\varepsilon-\beta\,\delta\,\eta\,\psi \\
 & -\beta\,\delta\,\eta\,\sigma-\beta\,\delta\,\eta\,\varsigma-\beta\,\delta\,\omega\,\psi-\beta\,\delta\,\omega\,\sigma-\beta\,\delta\,\omega\,\varsigma-\beta\,\delta\,\psi\,\sigma-\beta\,\delta\,\sigma^2-\beta\,\delta\,\sigma\,\varsigma+\delta\,\eta\,\mu\,\sigma+ \\
 & \delta\,\eta\,\mu\,\varrho-\delta\,\eta\,\mu\,\varepsilon+\delta\,\mu\,\omega\,\sigma+\delta\,\mu\,\omega\,\varrho-\delta\,\mu\,\omega\,\varepsilon+\delta\,\mu\,\sigma^2+\delta\,\mu\,\sigma\,\varrho-\delta\,\mu\,\sigma\,\varepsilon) \\
d_1 = & (\eta+\omega+\sigma)\,(\xi+\sigma)\,(\rho-1)\,(-\mu\,\rho\,\varepsilon+\beta\,\psi+\beta\,\sigma+\beta\,\varsigma-\mu\,\sigma-\mu\,\varrho+\mu\,\varepsilon)'\quad d_2 = c_2 \\
e_1 = & \phi\rho\beta(\xi+\sigma)(\delta+\sigma+\nu),\quad e_2 = d_2
\end{cases}
\tag{2.9a}
$$

The bifurcation coefficients a and b, at the centre manifold are computed using the non-negative left and right eigenvectors of system 2.9a. Also, the nonzero second order partial derivatives of the state variables, when evaluated using the quasi-lockdown measure (bifurcation parameter), determines the direction of bifurcation. This simplifies the bifurcation coefficient at the centre manifold with effect of quasi-lockdown policy as follows;

$$
\begin{cases}
a = 2v_2w_1w_2\frac{\partial^2 f_2(\kappa^*)}{\partial x_1\partial x_2} = 2v_2w_1w_2\kappa^* = 2v_2w_1w_2\frac{\rho\varepsilon+\sigma+\varrho-\varepsilon}{\beta(\alpha-\sigma)} < 0,\ \alpha < \sigma < \varepsilon(1-\rho)+\varrho \\
b = v_2w_1\frac{\partial^2 f_2(\kappa^*)}{\partial x_1\partial \kappa^*} + v_2w_2\frac{\partial^2 f_2(\kappa^*)}{\partial x_1\partial \kappa^*} = 2v_2\kappa^*(w_1+w_2) = 2v_2(w_1+w_2)\frac{\rho\varepsilon+\sigma+\varrho-\varepsilon}{\beta(\alpha-\sigma)} > 0, \\
where \\
\alpha < \sigma < \varepsilon(1-\rho)+\varrho
\end{cases}
\tag{3.0}
$$

Observe that the computed coefficient of bifurcation changes sign at the speed determine by quantity $\alpha < \sigma < \varepsilon(1-\rho)+\varrho$. Hence, the centre manifold theory depicts the existence of forward and transcritical bifurcation with forward hysteresis effects. Epidemiologically, the quasi-lockdown policy necessitated reduction in the sporadic spread of the disease, but not sufficient to extinct the virus from the system. This implies that restrictions such as schools closure, halting of major organizational gatherings (church and mosques), stoppage of clusters in market places and shutting down business premises had curtailed the spread of the infection, although the disease could persist endemically.

4.0 Computational Dynamics and Numerical Simulations

This section discusses data analysis with the help of simulation packages in maple16 software.

4.1 Estimation of Epidemiologic datasets using Nonlinear Regression Model

The observed datasets from NCDC are parameterized and fitted using nonlinear least Square regression for predictive and simulation purposes. The NLS regression model y = f(x) for a ten point datasets($n = 10$), were used to estimate unknown epidemiologic parameters Θ_i, which minimizing the values of the differences between the sum of squares of the observed datasets , and the fitted data ($y = f(x_i)$ as such that,

$$min\Theta_i = \sum_{i,j=1}^{n} [y_i - f(x_j)] \tag{3.1a}$$

$$R^2 = 1 - \frac{\sum\limits_{i=1^n} (y_i - \bar{y})^2}{\sum\limits_{i=1}^{2} y_i^2 - \frac{\sum\limits_{i=1}^{n} y_i^2}{n\left(\sum\limits_{i=1}^{n} y_i\right)^2}} \tag{3.1b}$$

$$f(x^*) \pm t_{\frac{\alpha}{2}} \frac{s}{\sqrt{n}} \left(1 + \frac{1}{n} + \frac{(x^* - \bar{x})}{\sum\limits_{i=1}^{n} (x_i - \bar{x})^2} \right), \quad \forall x^* \in x_i \tag{3.1c}$$

The least square minimizing function is given in equation 3.1a, coefficient of determination is given in 3.1b, and equation 3.1c depicts the predictable interval of the datasets within a 95% credibility at 0.05 level of significance. Its necessary to envisage that the closer the coefficient of determination R^2 to 1, the better the fitted datasets into the observed datasets. Table 1 reveals the observed datasets, peculiar to Akwa Ibom State as reported by NCDC. This shown the epic-weeks of the infection, weekly datasets, cumulative confirmed cases (CCC), recovery cases (RC), death case (RC), active active(AC), case fatality ratio (CFR), case recovery ratio (CRR) as shown in table 1.

Table 1: Weekly Report of COVID-19 Transmission Cases in 2021 in Akwa Ibom State, Nigeria

August to October 2021	Week	CCC	RC	DC	AC	CFR	CRR
9th to 15th August, 2021	32	3511	2650	32	829	0.9114	0.7548
16th to 22nd August, 2021	33	3739	2943	32	764	0.8558	0.7871
23rd to 29th August, 2021	34	3984	3200	42	742	1.0542	0.8032
30th Aug., to 5th Sept, 2021	35	4135	3355	42	738	1.0157	0.8114
6th to 12th Sept, 2021	36	4221	3534	42	645	0.9950	0.8372
13th to 19th Sept, 2021	37	4282	3647	42	593	0.9809	0.8517
20th to 26th Sept, 2021	38	4319	3714	42	563	0.97245	0.8599
27th Sept, to 3rd Oct, 2021	39	4335	3864	44	427	1.01499	0.8913
4th to 10th Oct, 2021	40	4342	3940	44	358	1.0134	0.9074
11th to 17th Oct, 2021	41	4346	3986	44	316	1.01242	0.9172

According to the Nigeria Centre of Disease Control ([NCDC], 2023), the spread of the infection was in its epi-week within 1st to 30th August, 2021. The dataset extracted within this time frame is shown in table 1, and were used for fitting parameters and estimation of state variable in the model. There are relatively good line of best fits as shown in figure 3. Figure 3 has relatively high coefficient of determination; $R^2 = 0.94$ on average.

Using the regression model, the average fatality rate and recovery rate of the infection were fitted as 0.98% and 0.84% respectively. This implies a low recovery rate and less than 1% chance of surviving after contacting the virus.

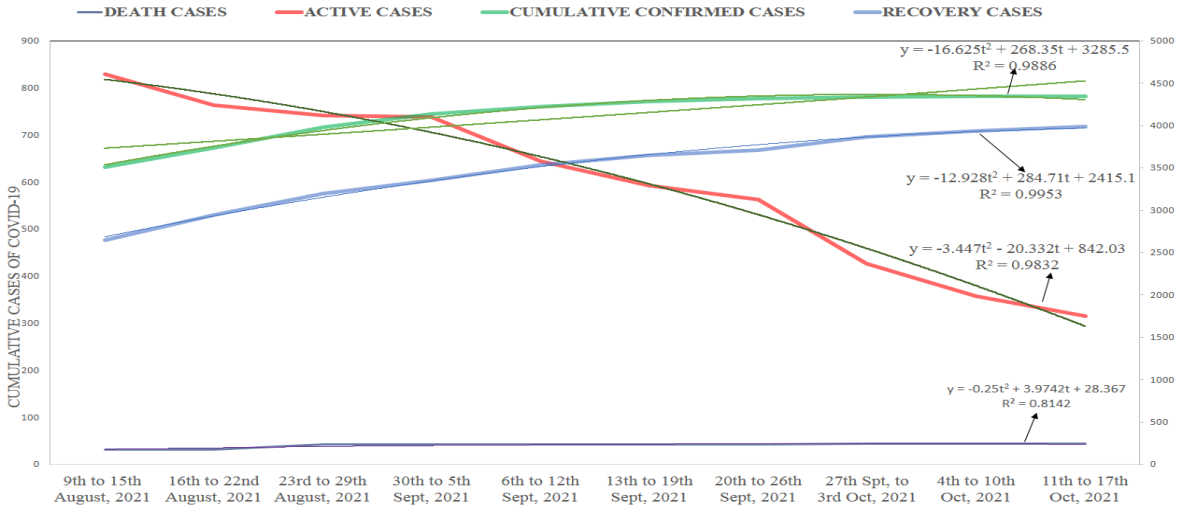

Figure 3: Lines of best fit of COVID-19 cases in epi-Weeks in Akwa Ibom (NCDC, 2023)

The estimated parameter values associated with 95% prediction intervals for compartmental population yields the result in table 2. Using the total population of people (National Bureau of Statistics [NBS], 2018) in Akwa Ibom state $4,987,740$ people, and before the quasi-lockdown policy, the susceptible population was estimated. The total intrinsic growth rate and recruitment of people into the susceptible class depends on the natural birth rate per woman per year in the entire population. Using the birth registration data $157,121$ in 2016, the natural birth rate and recruitment to the susceptible class, $\alpha = \frac{157121}{4987740} \times 100 = 4.15\%$. Since the estimated incubation period of the infection is between 13 days to 15 days, the effective progression rate ρ on average from exposed class to infected class is estimated as $\rho = \frac{1}{5.21 \times 14}$ per week. The average death rates in respective compartments, as well as the recovery rates are estimated within the interval $(0, 3]$ respectively. The natural death rates are equal in each compartment, and estimated using the life-expectancy. The life expectancy of adult individuals in Akwa Ibom state is approximated 52.1years, hence the natural death rate $\sigma = \frac{1}{52.11 \times 72}$ per week. On restrictions due to quasi-lockdown policy, the parameter κ is free and uncertain. Other parameters are estimated using validated results from the literature as see in table 2.

Table 2: Parameterization of COVID-19 epidemiologic variables

Meaning	Notations	Estimated values	RC Source
Susceptible class	$S(t_0)$	4.9×10^6	fitted
Exposed class	$E(t_0)$	***	estimated
Infected class	$I(t_0)$	3286	fitted
Asymptomatic infected class	$A(t_0)$	***	estimated
Hospitalized class	$H(t_0)$	842	fitted
Recovered class	$R(t_0)$	2415	fitted
Natural birth rate	α	10.5	estimated
Transmission rate from susceptible to exposed	β	1.75	estimated
Transmission rate from susceptible to infected	μ	1×10^{-6}	estimated
Transition rate from exposed to asymptomatic	ε	0.5	esitmated
Proportion of exposed that moved to infected	ρ	1.98	estimated
Transition rate from hospitalized to recovery	η	1.50	estimated
Recovery rate from asymotomatic(yeld immunity)	δ	1.5	estimated
Natural death rate	σ	0.02	estimated
Disease induced death rate of hospitalized	ω	2.5	estimated
Disease induced death rate of Asymptomatic	ν	1.22	estimated
Disease induced death rate of infected	ς	0.2235	estimated
Disease induced death rate of exposed	ϱ	2.005	estimated
Uncertain death rate after recovery	ξ	0.5	estimated
Quasi-lockdown measure	κ	$(0, \infty)$	controller

4.2 Sensitivity Analysis of Basic Reproduction Number (R_0)

A Normalized Forward Sensitivity Index(NFCI) is required to establish the computational fidelity of the model. Uncertainties, and effective changes of epidemiological parameters against the spread of the infection(basic reproduction number; R_0), and quasi-lockdown effect (κ) can be computed using NFCI. Consider a response function $R_0 = (F(X_p, p))$, where X_p is a parameter space, in respect to the parameter p, then the ratio of the relative changes in the response variable to the relative changes in the parameters, denoted as $S_p^{R_0} = \frac{\partial F}{\partial p}\frac{p}{R_0}$ defines the NFCI. In system (2.3), the basic reproduction number depends on parameters $(X_p = \beta, \alpha, \rho, \epsilon, \varepsilon, \sigma, \varrho)$. Applying this definition, the following indices were obtained, dependent on the basic reproduction number(R_0). Using table 3, the sign change of each sensitivity index predicts the direction of increase or decrease in the spread of the infection, dependent on parameter of interest. Clearly, table 3 shows that the quasi-lockdown policy(κ), and transition rate of susceptible to exposed class (β) yielded a significantly large effect size on the basic reproduction number(R_0) of the infection.

Table 3: Sensitive Indices of COVID-19 Parameters

Epidemiologic meaning	Paramters	Values	Sensitivity Indices
Natural birth rate	α	10.5	+0.001156
Natural death rate	σ	0.02	−0.0299
Transmission rate from susceptible to exposed	β	1.75	+1.0000
Transition rate from exposed to infected	ε	2.5	−0.6748
Proportion of exposed that moved to infected class	ρ	1.98	−1.3634
Disease induced death rate of exposed	ϱ	2.005	−0.3068
Quasi-lockdown measure(susceptibility capacity)	κ	3.77745	+1.0000

Figure 4 demonstrated a proportional increase in the spread of the infection, due to increase of influx of people by birth $\alpha = +ve$ to the susceptible class, and increase in the transmission rate $\beta = +ve$ from susceptible to exposed class. This implies that an increase of 10% of people by birth to the susceptible class will lead to

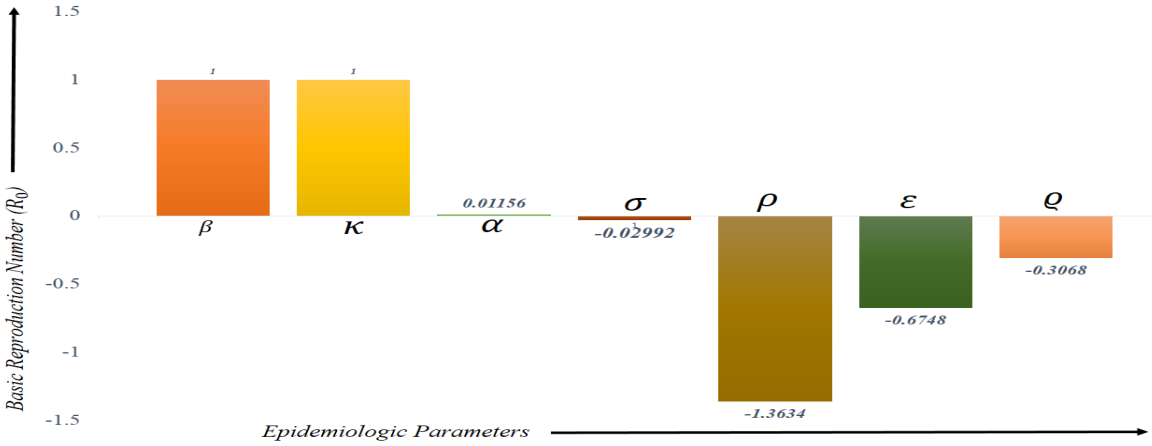

Figure 4: Tornado plot profile of COVID-19 sensitivity indices in Akwa Ibom State

an increase in 0.02% in the basic reproduction number R_0 of the infection. Similarly, an increase by 10% of the disease transmission rate to the exposed class, will leads to a corresponding increase in 10% of the basic reproduction number R_0 of the disease. Observe that, the quasi-lockdown measure $\kappa = +ve$ which signifies restriction of movement of susceptible class, can possibly increase the spread of the infection, when more people are allowed to interact. Empirically, an increase in number of susceptible persons by relaxation of the quasi-lockdown measure by 10%, will lead to a corresponding increase of 10% in the basic reproduction number R_0 of the disease. Consequently, other parameters of the basic reproduction number indicate an increasing trend of the basic reproduction number, when they are decreased. A contour map and phase space diagram is used to visualized the dynamics of the basic reproduction number R_0 plotted against other parameters.

4.3 Contour Maps of COVID-19 Basic Reproduction Number Against Sensitive Parameters

Contour maps and phase space diagram has been used to visualize the dynamical interactions between the basic reproduction number; R_0, and some sensitive parameters. Figure 6(a-i) illustrates the changes in basic reproduction(R_0) as plotted against the transition rate of susceptible class(β) to the exposed classed, as well as the effectiveness of the quasi-lockdown measure(κ).

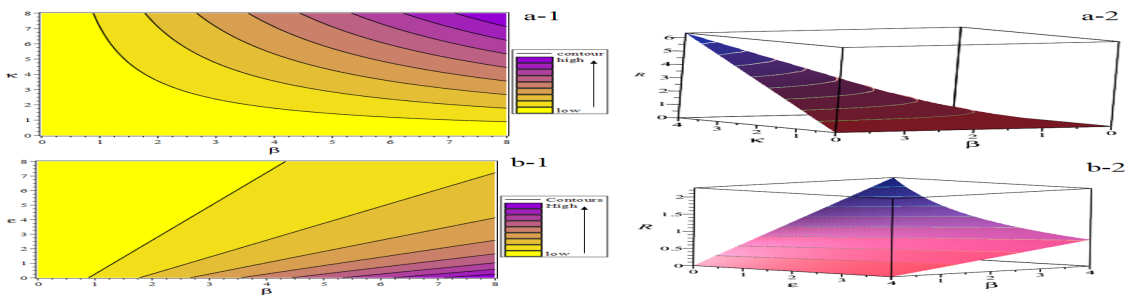

Figure 5: Contour and phase space diagram of R_0 against β , ε *and* κ

It shows that any increase in the population of the exposed class, increases the spread of the infection,and proportional increase in basic reproduction number (R_0). It's important to envisage that increasing the lockdown parameter implies increasing the susceptibility of the entire population to the disease. In figure 5(a-ii), relaxation of the lockdown policy or increasing the population of the susceptible class leads to a corresponding increase in the basic reproduction number(R_0). So, the partial lockdown policy assisted in curtailing the spread of the infection.

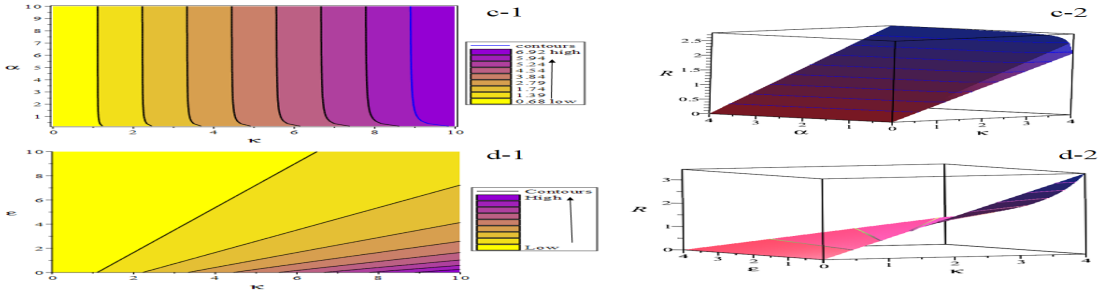

Figure 6: Contour and phase space diagram of R_0 against α, ε *and* κ

In Figure 5(b i and ii), the basic reproduction number is not sensitive to the transition rate of exposed to infected class, but sensitive to any increase in the infectivity of the susceptible class. Similar situation has been show in figure 6(c and d). This affirms the efficacy of restriction of susceptible class, through lockdown policy, as a major strategic to reduce the spread of the infection in the entire population.

4.4 Discussions of Dynamical Behaviours and Bifurcations at Equilibrium Points

Using the baseline epidemiologic datasets in table 2, the disease free equilibrium $E_0 \to (1.4829, 0, 0, 0, 0, 0)$, assumes asymptotically stable behaviour. This behaviour is possible when the quasi-lockdown policy $\kappa^* = 1.5$ was enforced strictly, and basic reproduction number $R_0 \leq 1$, $R_0^* = 0.3971 < 1$. This dynamics satisfies the conditions of theorem 4 since the characteristic polynomial;
$P(\lambda) = 250.2530 + 936.8059\lambda + 1219.9477\lambda^2 + 686.1668\lambda^3 + 183.9312\lambda^4 + 22.7435\lambda^5 + \lambda^6$,
yields negative eigenvalues;
$\lambda_1 = -3.94,\ \lambda_2 = -0.8435,\ \lambda_3 = -10.38,\ \lambda_5 = -2.84,\ \lambda_5 = -4.12,\ \lambda_6 = -0.620$
Hence the solution profile in figure 7, converges to a stable fixed point in the model. Similarly, the model

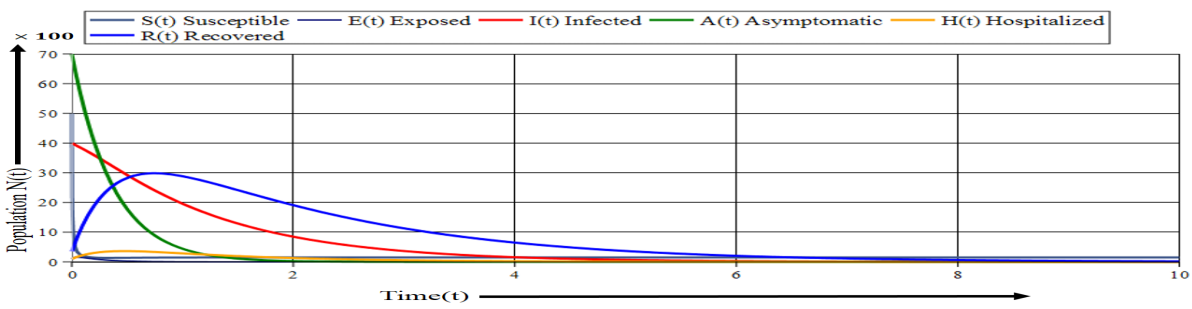

Figure 7: Stable dynamics at disease free equilibrium point

remains stable at the disease free equilibrium on small relaxation of the quasi-lockdown policy κ, say $\kappa^* \in (0, 3.77745]$, with basic reproduction number $R_0 < 1$. Otherwise it bifurcates from the stable manifold at $R_0 = 1$, and degenerates a transcritical dynamics (see figure 8). This satisfies the conditions of existence of forward bifurcation with hysteresis effect [23, 24, 25], and conditions in theorem 4, where the bifurcation coefficients $a = -0.1836 < 0$, $b = 0.054 > 0$ changes sign. Accordingly, stable(red line), and unstable(blue) oscillating endemic region emerged from the stable transient bifurcation point. Also, the disease free equilibrium spans to the unstable region(yellow asymptotic line) as seen in figure 8 below.

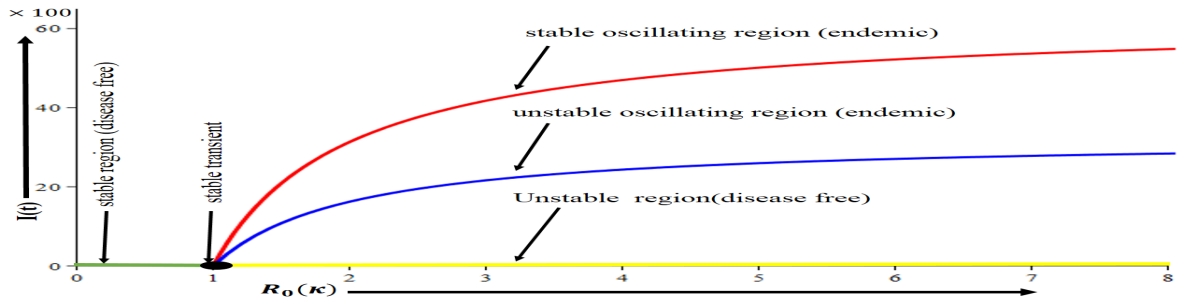

Figure 8: Diagram of forward and transcritical bifurcations at centre manifold $R_0 = 1$

These dynamics can be visualized using solution profiles at the endemic equilibrium points; stable and unstable oscillating solutions respectively. The oscillating solution converges to the stable endemic equilibrium point; $E_1 \to (S = 3.7343,\ E = 5.90898,\ I = 62.4185,\ A = 9.175575,\ H = 7.575062,\ R = 40.52574)$ as seen in figure 9.

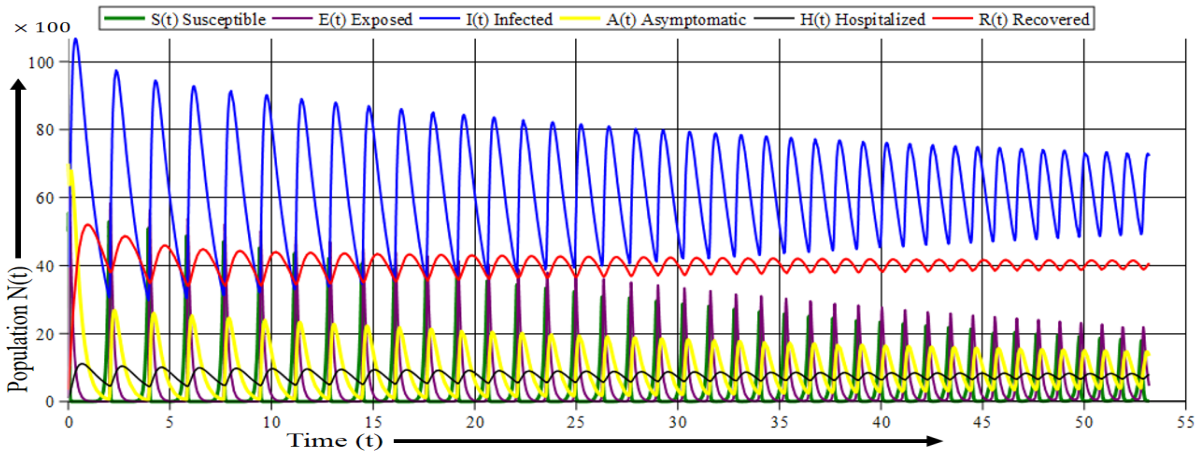

Figure 9: Stable oscillating solution profile at endemic equilibrium point (E_1)

These dynamics occur as the quasi-lockdown measure was relaxed ($\kappa^* \in (3.77745, 1000]$), at the endemic equilibrium point $E_1 \to (S = 3.7343, E = 5.90898, I = 62.4185, A = 9.175575171, H = 7.57506, R = 40.52573634)$. The dynamics satisfies local stability conditions, as negative eigenvalues occurs when evaluating the characteristic polynomial;
$P(\lambda) = (-67.60972778\lambda - 0.8826949142\lambda^2 - \lambda^3 - 57.00023298)(-2.84 - \lambda)(-4.12 - \lambda)(-.62 - \lambda)$,
at the endemic equilibrium point. The oscillating solution occurs in accordance with theorem 3, when the basic reproduction number $R_0 > 1$, say $R_0 = 265 \in (1, \infty)$. Subsequently, a further relaxation of the quasi-lockdown

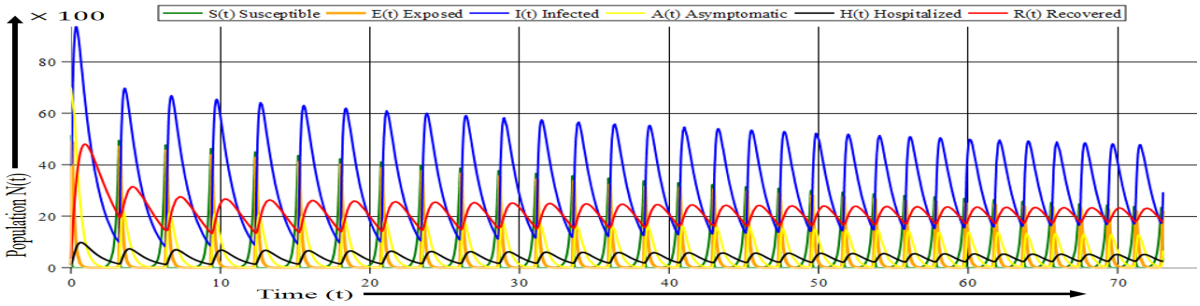

Figure 10: Unstable oscillating solution profile at endemic equilibrium point (E_1^*)

policy, say ($\kappa^* = 1000.15 \in (1000, \infty)$) yielded an unstable oscillating solution profile, which implies an existence of forward bifurcation with hysteresis effect(see figure 10). This oscillating dynamics is unstable at the endemic equilibrium point $E_1^* \to (S = 3.7342, E = 3.0625, I = 32.3505, A = 4.7555, H = 3.9260, R = 21.004)$, since at least one of the eigenvalues of the characteristic polynomial;
$P(\lambda) = 214.3144 - 19.0931\lambda^3 + 0.0308\lambda^4 - 84.657\lambda^2 - 2.2437 \times 10^{-9}\lambda^5 + \lambda^6 + 207.73492\lambda$,
given as ($2.6283 \pm 0.5997i,\ -0.7541 \pm 3.4331i,\ -2.93538,\ -0.8131$) has a non negative real part. Epidemiologically, the model predicted a negative impacts in the state, if there was a further relaxation of the quasi-lockdown policy.

5.0 Conclusion

In this research work, a compartmental populations of susceptible, exposed, infected, asymptomatic, hospitalized and recovered(SEIAHR) model has been designed to describe the dynamics of COVID-19 pandemic in Akwa Ibom State. The model incorporated a logistic function, as the per capita influx rate of the entire population to the susceptible class, with the carrying capacity as a measure of quasi-lockdown policy. Its investigated the effectiveness and impact of quasi-lockdown policy (a measure of strategic economy restrictions, and halting of human to human interactions of different forms within the state) to curtail the spread of the infection. The feasibility, well-possedness, existence and uniqueness of the model were established using fixed point theory. Qualitative dynamical behaviour of the model includes local stability at the pandemic free equilibrium, transcritical bifurcation, forward bifurcation with hysteresis effect(oscillating stable and unstable dynamics) as the disease persists endemically. The model demonstrated that the quasi-lockdown policy was necessarily effective to curtail the exponential spread of the infection in the population, when it was enforced strictly. On the other hand, the model predicted unstable oscillating behaviour when simulated using the baseline parameter on variation and relaxation of the quasi-lockdown policy. Thus we inferred that the quasi-lockdown policy was pseudo-effective in controlling virus development and spread, but a pre-mature lifting of the lockdown policy could have lead to disaster. Sophisticated and more robust techniques were recommended to the policy makers, such as vaccinations and treatments to facilitate optimal control and complete eradication of the plague in the state.

Supporting Organizations

The project was fully funded by TETfund using Institution Based Research grant (TETFUND/UNIUYO/IBR/2020), and partially by TetFund Centre of Excellence in Computational Intelligence Research, University of Uyo, Uyo.

Acknowledgements

The authors would like to express their sincere thanks to the editorials including all reviewers for their helpful comments and suggestions.

Competing Interests

Authors have declared that no competing interests exist.

References

[1] Shailendra K Saxena. Coronavirus disease 2019 (COVID-19): epidemiology, pathogenesis, di- agnosis, and therapeutics. Springer nature, 2020.

[2] L Kim, J Hayes, P Lewis, AV Parwani, KO Chang, and Linda Jean Saif. Molecular char- acterization and pathogenesis of transmissible gastroenteritis coronavirus (tgev) and porcine respiratory coronavirus (prcv) field isolates co-circulating in a swine herd. Archives of virology, 145:1133–1147, 2000.

[3] Lin Zhang, Jiahua Zhu, Xuyuan Wang, Juan Yang, Xiao Fan Liu, and Xiao-Ke Xu. Charac- terizing covid-19 transmission: incubation period, reproduction rate, and multiple-generation spreading. Frontiers in Physics, 8:589963, 2021.

[4] Joseph Bamidele Awotunde, Roseline Oluwaseun Ogundokun, Abidemi Emmanuel Adeniyi, Kazeem Moses Abiodun, and Gbemisola Janet Ajamu. Application of mathematical modelling approach in covid-19 transmission and interventions strategies. In Modeling, Control and Drug Development for COVID-19 Outbreak Prevention, pages 283–314. Springer, 2022.

[5] S Olaniyi, OS Obabiyi, KO Okosun, AT Oladipo, and SO Adewale. Mathematical modelling and optimal cost-effective control of covid-19 transmission dynamics. The European Physical Journal Plus, 135(11):938, 2020.

[6] RH Huang, DJ Liu, J Guo, JF Yang, JH Zhao, XF Wei, S Knyazeva, M Li, RX Zhuang, CK Looi, et al. Guidance on flexible learning during campus closures: Ensuring course quality of higher education in covid-19 outbreak. Beijing: Smart Learning Institute of Beijing Normal University, 2020.

[7] Ronghuai Huang, DJ Liu, Ahmed Tlili, JunFeng Yang, HuaHaun Wang, et al. Handbook on fa- cilitating flexible learning during educational disruption: The chinese experience in maintaining undisrupted learning in covid-19 outbreak. Beijing: Smart Learning Institute of Beijing Normal University, 46, 2020.

[8] Nicolas Reuge, Robert Jenkins, Matt Brossard, Bobby Soobrayan, Suguru Mizunoya, Jim Ack- ers, Linda Jones, and Wongani Grace Taulo. Education response to covid 19 pandemic, a special issue proposed by unicef: Editorial review. International Journal of Educational Development, 87:102485, 2021.

[9] Paul Ani Onuh. Nigeria's response to covid-19: Lockdown policy and human rights violations. African Security, 14(4):439–459, 2021.

[10] Joshua, E. E., Akpan, E. T., Inyang, U. G. (2024). Computational Nonlinear Dynamics: Analysis and Assessment in Optimal Control of COVID-19 in Akwa Ibom State, Nigeria. Journal of Advances in Mathematics and Computer Science, 39(1), 1–19. https://doi.org/10.9734/jamcs/2024/v39i11858

[11] oh Iwasa, Akane Hara, and Shihomi Ozone. Virulence of a virus: How it depends on growth rate, effectors, memory cells, and immune escape. Journal of Theoretical Biology, 530:110875, 2021.

[12] Ronghuai Huang, DJ Liu, Ahmed Tlili, JunFeng Yang, HuaHaun Wang, et al. Handbook on fa- cilitating flexible learning during educational disruption: The chinese experience in maintaining undisrupted learning in covid-19 outbreak. Beijing: Smart Learning Institute of Beijing Normal University, 46, 2020.

[13] Shikha Saha and Amit Kumar Saha. Modeling the dynamics of covid-19 in the presence of delta and omicron variants with vaccination and non-pharmaceutical interventions. Heliyon, 9(7), 2023.

[14] Sarbaz HA Khoshnaw, Kawther Yusuf Abdulrahman, and Arkan N Mustafa. Impact of vac- cination strategies on the spread of covid-19 pandemics: A mathematical modelling approach. 2023.

[15] Shasha Gao, Pant Binod, Chidozie Williams Chukwu, Theophilus Kwofie, Salman Safdar, Lora Newman, Seoyun Choe, Bimal Kumar Datta, Wisdom Kwame Attipoe, Wenjing Zhang, and P. van den Driessche. A mathematical model to assess the impact of testing and isolation compliance on the transmission of covid-19. Infectious Disease Modelling, 8(2):427–444, 2023.

[16] Eleftheria Tzamali, Vangelis Sakkalis, Georgios Tzedakis, Emmanouil G Spanakis, and Nikos Tzanakis. Mathematical modeling evaluates how vaccinations affected the course of covid-19 disease progression. Vaccines, 11(4):722, 2023.

[17] Mayowa M. Ojo, Olumuyiwa James Peter, Emile Franc Doungmo Goufo, and Kottakkaran Sooppy Nisar. A mathematical model for the co-dynamics of covid-19 and tuberculosis. Mathematics and Computers in Simulation, 207:499–520, 2023.

[18] Zenebe Shiferaw Kifle and Legesse Lemecha Obsu. Co-dynamics of covid-19 and tb with covid-19 vaccination and exogenous reinfection for tb: An optimal control application. Infectious Disease Modelling, 8(2):574–602, 2023.

[19] Morris W Hirsch, Stephen Smale, and Robert L Devaney. Differential equations, dynamical systems, and an introduction to chaos. Academic press, 2012.

[20] Manotosh Mandal, Soovoojeet Jana, Sayani Adak, Anupam Khatua, and Tapan Kumar Kar. A model-based analysis to predict and control the dynamics of covid-19. Modeling, Control and Drug Development for COVID-19 Outbreak Prevention, pages 87–118, 2022.

[21] E. T. Akpan, E. E Joshua, and E. I Uduk. Nonlinear dynamics and synchronization of computational cognitive model in educational sciences. J. Nonlinear Sci. Appl, 14(1):15–28, 2020.

[22] Carlos Castillo-Chavez and Baojun Song. Dynamical models of tuberculosis and their applications. Math. Biosci. Eng, 1(2):361–404, 2004.

[23] Lin Zhang, Jiahua Zhu, Xuyuan Wang, Juan Yang, Xiao Fan Liu, and Xiao-Ke Xu. Characterizing covid-19 transmission: incubation period, reproduction rate, and multiple-generation spreading. Frontiers in Physics, 8:589963, 2021.

[24] Lawrence Perko. Differential equations and dynamical systems, volume 7. Springer Science & Business Media, 2013.

[25] Jayanta Kumar Ghosh and Uttam Ghosh. Three dimensional epidemic model with non- monotonic incidence and saturated treatment: a case study of sars infection of hong kong 2003 scenario. Results in Control and Optimization, page 100239, 2023.